厚生労働科学研究費補助金

萌芽的先端医療技術推進研究事業

細胞内動態制御機能を有する新規細胞選択型ナノ遺伝子キャリアの開発と遺伝子治療への応用

平成１７年度　総括研究年度終了報告書

主任研究者　　川上　茂

平成１８（２００６）年　４月

目　　次

厚生労働科学研究費補助金（萌芽的先端医療技術推進研究事業）
研究報告書

細胞内動態制御機能を有する新規細胞選択型ナノ遺伝子キャリアの開発と遺伝子治療への応用

主任研究者　川上　茂　京都大学大学院薬学研究科

研究要旨　本研究は、生体内で細胞特異的デリバリーなど高度な機能を発揮する多機能性標的指向型ナノ・遺伝子キャリアの創製を行うため、細胞特異的認識素子の表面導入、あるいは細胞内動態制御の指針となる総合的な設計戦略を確立し、同時に実用性の高い *in vivo* レベル遺伝子発現制御技術の開発を目指す。さらに本研究を通して開発した新規多機能性標的指向型ナノ・遺伝子キャリアを遺伝子治療へと応用する。本年度は、新規ガラクトース (Gal-)ならびにマンノース(Man-)-ヒスチジン (His) 修飾リポソーム複合体の物理化学的性質、細胞への取り込み特性ならびに遺伝子発現能、マウスへ *in vivo* 投与後の遺伝子発現の評価をおこなった。Gal-, Man-His-C4-Chol 含有リポプレックスの平均粒子径ならびにゼータ電位は、100 - 120 nm、60 - 65 mV であり、His 導入によりこれら物理化学的性質に大きな変化はみられなかった。アシアロ糖タンパク質レセプターを高発現するヒト肝臓癌由来細胞株 HepG2 細胞を用いて細胞取り込みならびに遺伝子発現を評価したところ、細胞取り込みはほぼ同程度であったが、His 導入により遺伝子発現は有意に増大し、His 導入による細胞内動態が遺伝子発現増大に関係していることが示唆された。さらに Gal-His-C4-Chol 含有リポソーム複合体の細胞取り込みならびに遺伝子発現は、過剰量のガラクトース共存により有意な低下し、アシアロ糖タンパク質レセプターによる細胞取り込みの可能性が示された。また *in vivo* での応用に関して、腹腔内投与が血管内投与に比べ生体成分との相互作用も少なく、腹腔およびリンパ内抗原提示細胞への遺伝子導入に適していると考えられる。そこで、His を含有しない従来の Man-C4-Chol 含有リポソーム複合体を腹腔内投与したところ、抗原提示細胞への効率的な遺伝子導入ならびに強力な細胞障害性 T 細胞の誘導が示された。さらに、Man-His-C4-Chol 含有リポソーム複合体を腹腔内投与により、*in vivo* において遺伝子発現を改善できることが示された。

A.　研究目的

本研究は、生体内で細胞特異的デリバリーなど高度な機能を発揮する多機能性標的指向型ナノ・遺伝子キャリアの創製を行うため、細胞特異的認識素子の表面導入、あるいは細胞内動態制御の指針となる総合的な設計戦略を確立し、同時に実用性の高い *in vivo* レベル遺伝子発現制御技術の開発を目指す。具体的には、i)新規細胞内動態制御型遺伝子導入キャリアの開発、ii) *in vivo* 細胞特異的遺伝子導入のための製剤設計を通じて、最終的には iii) DNA ワクチン療法等の遺伝子治療への応用を目指す。

B.　研究方法

Man/Gal-His-C4-Chol 合成: 平成16年度総括報告書に報告した方法により合成した。リポソームの調製: DOTMA/cholesterol/Man-His-C4-Chol をモル比 1:0.5:0.5 の割合で混合し、vortex 法により調製した。物理化学的性質の測定:ゼータ電位および平均粒子径は動的光散乱法により測定した。*In vivo* 遺伝子導入の評価: 5 週齢雌性 ICR マウス（22 – 25 g）の門脈あるいは腹腔内へ各種複合体 (p-CMV-Luc; 30 or 50 μg) を投与した。マウスを安楽死させ、肝臓、肺、あるいは腹腔滲出細胞（APCs)、大網、リンパ節を回収し、それぞれの細胞における遺伝子発現レベルを測定した。細胞障害性 T 細胞（CTL）誘導の評価: 腹腔内または筋肉内投与投与後、脾臓細胞を B16BL6 細胞と共存下にて培養し、B16BL6 細胞に対して CTL の評価をおこなった。

C.D. 結果・考察

i) 新規細胞内動態制御型遺伝子導入キャリアの開発: His を含む新規 Gal-His-C4-Chol 含有リポソームの平均粒子径・ゼータ電位ともに対照のリポプレックス群とほぼ同じ値であった。次に、^{32}P 標識した pDNA を用

いてアシアロ糖タンパクレセプターを高発現するHepG2細胞への取り込みを評価した結果、高い取り込みを示すことが明らかとなった。次に、HepG2細胞への遺伝子導入能を評価した結果、Gal-His-C4-Chol含有リポプレックスは、有意に高い遺伝子発現能を示した。また、細胞取り込みと遺伝子発現の相関より、Gal-His-C4-Chol含有リポソーム複合体はアシアロ糖タンパクレセプターにより細胞選択的に取り込まれ、細胞内動態の改善により高い遺伝子発現に至っていることが示された。*in vivo*における遺伝子導入能を評価するため、門脈内投与により各種リポプレックスを投与した。アシアロ糖タンパクレセプターが高発現する肝臓において有意に高い遺伝子発現が認められ、新規機能性脂質含有リポソームは*in vivo*においても利用可能な遺伝子キャリアであることが示された。同様にMan-His-C4-Chol含有リポソーム複合体は、腹腔内投与によりマンノースレセプターを介した細胞選択的な取り込みにより効率的な抗原提示細胞への遺伝子導入が可能であることを明らかにした。以上、Gal-およびMan-His-C4-Chol含有リポソームが有用な多機能型遺伝子導入キャリアとなり得ることが示された。

ii) *in vivo*遺伝子導入のための製剤設計: 血管内へカチオン性リポソーム複合体を静脈内投与後、主に赤血球との相互作用により標的細胞へのデリバリーが阻害されていることを明らかにした。一方、中性脂質として広く用いられるpH感受性脂質DOPEを含有するリポソーム複合体は静脈内投与後肺からの脱出が早く、肺以外の臓器へのターゲティングに適していることが示唆された。また、腹腔内は生体成分も血管内と比べて少なく、腹腔内やリンパに存在する抗原提示細胞への長期的かつ効率的な遺伝子導入が可能であることを明らかにした。一方、腹腔内投与ではDOPEを含むカチオン性リポソーム複合体の遺伝子導入能は低く、cholesterolを用いてリポソーム膜を安定化させることで遺伝子発現を改善できることが示唆された。さらに、複合体形成時の溶媒のイオン濃度が安定な複合体形成に重要であり、*in vivo*遺伝子導入能にも影響することを明らかにした。以上、静脈内投与ならびに腹腔内投与における遺伝子導入におよぼす製剤学的な因子を明らかにした。

iii) 遺伝子治療への応用: ii)での解析に基づき、腹腔内投与による抗原提示細胞デリバリーに基づくDNAワクチン療法の開発をおこなった。その結果、マンノース修飾リポソーム複合体の腹腔内投与法による遺伝子導入法では、効率的な導入抗原特異的なCTL誘導に基づくがん免疫療法が可能であることを明らかにした。

E. 結論

Gal-, Man-His-C4-Chol含有リポソームが、有効な多機能性標的指向型ナノ・遺伝子キャリアとなり得ることが示された。また、効率的な*in vivo*遺伝子導入法の為の製剤学設計指針を明らかにした。さらに、DNAワクチン療法に基づく遺伝子治療が可能であることが示された。次年度はこれまでに得られた各種条件を基に、より安全かつ有効な遺伝子治療システムの実現を目指す。

F. 健康危険情報

なし

G. 研究発表

1. 論文発表

1) C. Managit, **S. Kawakami**, F. Yamashita, M. Hashida; Uptake characteristics of galactosylated emulsion by HepG2 hepatoma cells, *Int. J. Pharm.*, **301** (1-2), 255-261 (2005)

2) C. Managit, **S. Kawakami**, F. Yamashita, M. Hashida; Effect of galactose density on asialoglycoprotein receptor-mediated uptake of galactosylated liposomes, *J. Pharm. Sci.*, **94** (10), 2266-2275 (2005)

3) Y. Arakawa, **S. Kawakami**, F. Yamashita, M. Hashida: Effect of low-molecular-weight β-cyclodexrin polymer on release of drugs from mucoadhesive buccal firm dosage forms, *Biol. Pharm. Bull.*, **28** (9), 1679-1683 (2005)

4) Y. Higuchi, **S. Kawakami**, M. Nishikawa, F. Yamashita, M. Hashida: Intracellular distribution of NFκB decoy and its inhibitory effect on TNFα production by LPS stimulated RAW 264.7 cells, *J. Control. Release*, **107** (2), 373-382 (2005)

5) S. Fumoto, **S. Kawakami**, K. Shigeta, Y. Higuchi, F. Yamashita, M. Hashida: Interaction with blood components is a crucial role in asialoglycoprotein receptor-mediated *in vivo* gene transfer by galactosylated lipoplex, *J Pharmacol. Exp. Ther.*, **315** (2), 484-493 (2005)

6) Y. Hattori, S. Suzuki, **S. Kawakami**, F. Yamashita, M. Hashida: The role of

dioleoylphosphatidylethanolamine (DOPE) for targeted *in vivo* gene transfer to liver non-parenchymal cells following intravenous administration of mannosylated cationic liposomes, *J. Control. Release*, **108** (2-3), 484-495 (2005)

7) **S. Kawakami**, P. Opanasopit, M. Yokoyama, N. Chansri, T. Yamamoto, T. Okano, F. Yamashita, M. Hashida: Biodistribution characteristics of all-*trans* retinoic acid incorporated in liposomes and polymeric micelles following intravenous administration, *J. Pharm. Sci.*, **94** (12), 2606-2615 (2005)

8) W. Yeeprae, **S. Kawakami**, Y. Higuchi, F. Yamashita, M. Hashida: Biodistribution characteristics of mannosylated and fucosylated O/W emulsions in mice, *J. Drug Target.*, **13** (6), 1-9 (2005)

9) **S. Kawakami**, Y. Ito, S. Fumoto, F. Yamashita, M. Hashida: Enhanced gene expression in lung by a stabilized lipoplex using sodium chloride for complex formation, *J. Gene Med.*, 7 (12), 1526-1533 (2005)

10) **S. Kawakami**, S. Suzuki, F. Yamashita, M. Hashida: Induction of apoptosis in A549 human lung cancer cells by all-*trans* retinoic acid incorporated in DOTAP/cholesterol liposomes, *J. Control. Release*, **110** (3), 514-521 (2006)

11) M. Hashida, **S. Kawakami**, F. Yamashita: Lipid carrier systems for targeted drug and gene delivery, *Chem. Pharm. Bull.* **53** (8), 871-880 (2005)

12) **S. Kawakami**, M. Hashida: In vivo gene transfer by ligand-modified gene carriers, *Non-viral Gene Therapy*, K. Taira, K. Kataoka, T. Niidome (Ed.) Springer, Tokyo, pp. 226-236 (2005)

13) T. Okuda, **S. Kawakami**, M. Hashida: Evaluation of gene expression *in vivo* after intravenous and intraportal administration of lipoplex, *Non-viral Gene Therapy*, K. Taira, K. Kataoka, T. Niidome (Ed.) Springer, Tokyo, pp. 323-330 (2005)

14) **S. Kawakami**, F. Yamashita, M. Hashida: Liposomal *in vivo* gene delivery, *Modern Biopharmaceuticals*, Jörg Knäblein (Ed.), Wiley-VCH, Verlag GmbH & Co. KgaA, Weinheim, pp. 1507-1519 (2005)

2. **学会発表**

1) **川上　茂**、伊藤佳孝、山下富義、橋田　充: リポプレックスおよびポリプレックスの静脈内投与による免疫応答の評価、日本薬剤学会 20 周年記念大会、2005 年 3 月 25－27 日、東京.

2) **川上　茂**、服部芳幸、中村和美、山下富義、橋田　充: DNA ワクチン療法のためのマンノース修飾リポソームの開発、日本薬学会第 125 年会、2005 年 3 月 29－31 日、東京.

3) **川上　茂**、樋口ゆり子、山下富義、橋田充: Kupffer 細胞指向型ナノ微粒子の構築と核酸医薬品療法への応用、ナノ学会第 3 回大会、2005 年 5 月 8－10 日、仙台.

4) 重田耕佑、**川上　茂**、山下富義、橋田　充: プロトンスポンジ機能を有する新規ガラクトース修飾リポソームを用いた遺伝子導入能の評価、第 21 回日本 DDS 学会、2005 年 7 月 22－23 日、佐世保.

5) **川上　茂**、山下富義、橋田　充: 糖修飾リポソームを用いた遺伝子デリバリーと治療への応用、第 21 回日本 DDS 学会、2005 年 7 月 22－23 日、佐世保.

6) **川上　茂**、山下富義、橋田　充: 糖修飾カチオン性リポソームを用いた遺伝子・核酸医薬品の細胞選択的デリバリー、第 54 回高分子討論会、2005 年 9 月 20－22 日、山形.

7) **川上　茂**: リポソームによる遺伝子・核酸医薬品の細胞特異的ターゲティング、第 1 回創剤フォーラム若手発表会、2005 年 9 月 29－30 日、東京.

8) **S. Kawakami**: Mannosylated cationic liposomes for DNA vaccine therapy, the 8 th US-Japan symposium on drug delivery systems, 2005 年 12 月 18－22 日, Maui, USA.

9) **川上　茂**、橋田　充：ドラッグデリバリー、第 56 回医用高分子研究会、2006 年 3 月 8 日、東京.

H. **財産権の出願・登録状況**

1. 特許取得

1) **川上　茂**、橋田　充、嶋本　顕、高木基樹、佐藤あゆみ：肝指向性リポソーム組成物：(特願 2005-308288)、出願人：国立大学法人京都大学、ジーンケア研究所

2) **川上　茂**、橋田　充、樋口ゆり子: 免疫担当細胞指向型オリゴヌクレオチド・リポソーム複合体（特願 2005-008307)、出願人：国立大学法人京都大学

2. 実用新案登録　なし

3. その他　なし

雑誌

発表者氏名	論文タイトル名	発表誌名	巻号	ページ	出版年
S. Kawakami S. Suzuki F. Yamashita M. Hashida	Induction of apoptosis in A549 human lung cancer cells by all-*trans* retinoic acid incorporated in DOTAP/cholesterol liposomes	Journal of Controlled Release	110(3)	514-521	2006
S. Fumoto S. Kawakami K. Shigeta Y. Higuchi F. Yamashita M. Hashida	Interaction with blood components plays a crucial role in asialoglycoprotein receptor-mediated *in vivo* gene transfer by galactosylated lipoplex	Journal of Pharmacology and Experimental Theraputics	315(2)	484-493	2005
W. Yeeprae S. Kawakami Y. Higuchi F. Yamashita M. Hashida	Biodistribution characteristics of mannosylated and fucosylated O/W emulsions in mice	Journal of Drug Targeting	13(8-9)	479-487	2005
Y. Hattori S. Suzuki S. Kawakami F. Yamashita M. Hashida	The role of dioleoylphosphatidylethanolamine (DOPE) in targeted gene delivery with mannosylated cationic liposomes via intravenous route	Journal of Controlled Release	108(2-3)	484-495	2005
Y. Higuchi S. Kawakami M. Nishikawa F. Yamashita M. Hashida	Intracellular distribution of NFκB decoy and its inhibitory effect on TNFα production by LPS stimulated RAW 264.7 cells	Journal of Controlled Release	107(2)	373-382	2005
S. Kawakami P. Opanasopit M. Yokoyama N. Chansri T. Yamamoto T. Okano F. Yamashita M. Hashida	Biodistribution characteristics of all-*trans* retinoic acid incorporated in liposomes and polymeric micelles following intravenous administration	Journal of Pharmaceutical Sciences	94(12)	2606-2615	2005
S. Kawakami Y. Ito S. Fumoto F. Yamashita M. Hashida	Enhanced gene expression in lung by a stabilized lipoplex using sodium chloride for complex formation	Journal of Gene Medicine	7(12)	1526-1533	2005
C. Managit S. Kawakami F. Yamashita M. Hashida	Effect of galactose density on asialoglycoprotein receptor-mediated uptake of galactosylated liposomes	Journal of Pharmaceutical Sciences	94(10)	2266-2275	2005
C. Managit S. Kawakami F. Yamashita M. Hashida	Uptake characteristics of galactosylated emulsion by HepG2 hepatoma cells	International Journal of Pharmaceutics	301(1-2)	255-261	2005
Y. Arakawa S. Kawakami F. Yamashita M. Hashida	Effect of low-molecular-weight β-cyclodextrin polymer on release of drugs from mucoadhesive buccal film dosage forms	Biological & Pharmaceutical Bulletin	28(9)	1679-1683	2005
M. Hashida S. Kawakami F. Yamashita	Lipid carrier systems for targeted drug and gene delivery	Chemical & Pharmaceutical Bulletin	53(8)	871-880	2005

S. Kawakami M. Hashida	*In vivo* gene transfer by ligand-modified gene carriers	Non-viral Gene Therapy (Ed. K.Taira, K.Kataoka, T. Niidome)		226-236	2005
T. Okuda S. Kawakami M. Hashida	Evaluation of gene expression *in vivo* after intravenous and intraportal administration of lipoplexes	Non-viral Gene Therapy (Ed. K.Taira, K.Kataoka, T. Niidome)		323-330	2005
S. Kawakami F. Yamashita M. Hashida	Liposomal *in vivo* gene delivery	Modern Biopharmaceuticals (Ed. J Knäblein)		1507-1519	2005

Available online at www.sciencedirect.com
SCIENCE DIRECT
ELSEVIER
Journal of Controlled Release 110 (2006) 514–521
journal of controlled release
www.elsevier.com/locate/jconrel

Induction of apoptosis in A549 human lung cancer cells by all-*trans* retinoic acid incorporated in DOTAP/cholesterol liposomes

Shigeru Kawakami, Sachiko Suzuki, Fumiyoshi Yamashita, Mitsuru Hashida *

Department of Drug Delivery Research, Graduate School of Pharmaceutical Sciences, Kyoto University, Sakyo-ku, Kyoto 606-8501, Japan

Received 20 July 2005; accepted 31 October 2005
Available online 19 December 2005

Abstract

All-*trans* retinoic acid (ATRA) has been shown to exert anti-cancer activities in a number of types of cancer cells. However, it has been reported that many NSCLC exhibited resistance to ATRA treatment. In the present study, we hypothesized that intracellular delivery of ATRA would overcome the ATRA resistance in A549 cells. Here, we investigated the induction of apoptosis by ATRA incorporated in cationic liposomes composed of DOTAP/cholesterol in A549 human lung cancer cells, which are insensitive (resistant) to the growth inhibitory effects of ATRA. The zeta potentials of DOTAP/cholesterol liposomes and DSPC/cholesterol liposomes were about +50 and −3 mV. In A549 cells, [^{3}H]ATRA incorporated in DOTAP liposomes showed increased cellular association compared with [^{3}H]ATRA or [^{3}H]ATRA incorporated in DSPC/cholesterol liposomes. ATRA incorporated in DOTAP/cholesterol liposomes showed much higher cytotoxic effects and apoptosis-inducing activity compared with ATRA or ATRA incorporated in DSPC/cholesterol liposomes. The enhanced expression of TIG3 mRNA tumor suppressor gene by ATRA incorporation into DOTAP/cholesterol liposomes might partly explain the mechanism of enhanced cytotoxicity and/or apoptosis. These observations provide valuable information to help in the design of differentiation therapy by ATRA in non-small cell lung carcinoma.

Keywords: Cationic liposomes; All-*trans* retinoic acid; Non-small cell lung carcinoma; Drug delivery system

1. Introduction

Differentiation therapy in oncology is defined as an approach to induce malignant reversion [1] that is based on the concept that cancer cells are normal cells that have been arrested at an immature or less differentiated state, lack the ability to control their own growth, and so multiply at an abnormally fast rate. Although differentiation therapy does not kill the cancer cells, it restrains their growth and allows the application of more conventional therapies (such as chemotherapy) to eradicate the malignant cells. Moreover, differentiation agents tend to be less toxic than conventional cancer treatment.

Several groups have demonstrated that all-*trans* retinoic acid (ATRA) can induce complete remission in a high proportion of acute promyelocytic leukemia patients [2,3]. ATRA has been shown to exert anti-cancer activities in a number of types of cancer cells [4–8]. The activity of ATRA is mediated by regulation of a variety of forms of gene expression through ATRA-dependent activation of retinoic acid receptors (RAR) and retinoid X receptors (RXR) on the nuclear membrane of cancer cells, leading to the growth inhibition, differentiation, and apoptosis of cancer cells [9]. Response of non-small cell lung carcinoma (NSCLC) to ATRA is modulated by additional factors. Recently, a novel retinoid-regulated gene, tazorotene-induced gene 3 (TIG3), also called retinoic acid receptor responder, has been cloned and characterized [10]. Since TIG3 has been identified as a potential tumor suppressor [10–12], TIG3 could be a biomarker for response to ATRA as well as a mediator of the antitumor effect of ATRA in NSCLC.

However, it has been reported that many NSCLC exhibit resistance to ATRA treatment [12–15]. In order to achieve successful cancer differentiation therapy against NSCLC, ATRA resistance needs to be overcome. One strategy to overcome ATRA resistance involves the development of an ATRA delivery carrier to the NSCLC. The lipophilicity of

Abbreviations: DOTAP, 1,2dioleoyl-3-trimethylammonium propane; DSPC, distearoylphosphatidylcholine.

* Corresponding author. Tel.: +81 75 753 4525; fax: +81 75 753 4575.
E-mail address: hashidam@pharm.kyoto-u.ac.jp (M. Hashida).

0168-3659/$ - see front matter © 2005 Elsevier B.V. All rights reserved.
doi:10.1016/j.jconrel.2005.10.030

ATRA is too high (logPCoct (the logarithmic *n*-octanol/water partition coefficient) = 6.6) for efficient diffusion to the cellular membrane [16]; thus, it is quite likely that the cellular concentration for the action of ATRA is limited by its high lipophilicity. These observations prompted us to investigate whether the enhanced cellular uptake of ATRA by a drug carrier could be an efficient strategy to overcome ATRA resistance in NSCLC.

We have confirmed that most ATRA are incorporated in neutral liposomes due to their highly lipophilicity [17]. ATRA contain a carboxyl group; thus, ATRA would be more stably incorporated in cationic liposomes. Cationic liposomes are selectively accumulated in angiogenic endothelial cells in tumors [18] and remain largely confined to the tumor site compared with anionic or neutral liposomes after intravenous injection [19]. We have demonstrated that 50% of cationic liposomes composed of DOTAP/cholesterol accumulate in the lung 1 min after intravenous injection [20]. Cationic liposomes are internalized by endocytosis in these cells. Taking these findings into consideration, DOTAP/cholesterol liposomes are expected to be an effective drug carrier of ATRA for intracellular-NSCLC-selective delivery to overcome ATRA resistance in NSCLC.

In the present study, we investigated the induction of apoptosis by ATRA incorporated in DOTAP/cholesterol liposomes in A549 human lung cancer cells, which are insensitive (resistant) to the growth inhibitory effects of ATRA [12,14,15]. After application of ATRA incorporated in DOTAP/cholesterol liposomes in A549 cells, the cellular uptake mechanism, cytotoxicity, induction of apoptosis, and TIG3 mRNA expression were evaluated. Results were compared with free ATRA or ATRA incorporated in neutral liposomes (DSPC/cholesterol liposomes).

2. Materials and methods

2.1. Materials

DOTAP, DSPC, were obtained from Avanti Polar Lipids, Inc. (Alabaster, AL, USA) and Sigma-Aldrich Co. (St. Louis, MO, USA). Chol and Clear-Sol I were obtained from Nacalai Tesque, Inc. (Kyoto, Japan), and Soluene 350 was purchased from Packard Co., Inc. (Groningen, The Netherlands). Dulbecco's modified Eagle's minimum essential medium (DMEM) and fetal bovine serum (FBS) was obtained from Nissui Pharmaceutical Co., Ltd. (Tokyo, Japan) and Biowhittaker (Walkersville, MD, USA). ATRA and [^{3}H]ATRA was purchased from Wako Pure Chemicals Industry, Ltd. (Osaka, Japan) and NEN Life Science Products, Inc. (Boston, USA). MagExtractor-RNA kit was obtained from Toyobo Co., Ltd. (Osaka, Japan). SYBR-Green I was purchased from Takara Bio, Inc. (Shiga, Japan). All other chemicals were of the highest purity available.

2.2. Cell line

A549 cells were routinely grown in DMEM medium supplemented with 10% FBS, 100 IU/ml penicillin, 100 μg/ml streptomycin, and 2 mM L-glutamine (all from Invitrogen Co., Carlsbad, CA, USA) in 5% CO_2, humidified air at 37 °C.

2.3. Preparation of liposomes

Liposomes were prepared by the method described previously [21,22]. Briefly, DOTAP, DSPC and cholesterol were used to prepare the liposomes. The liposomes, DOTAP/cholesterol (1:1, molar ratio) and DSPC/cholesterol (3:2, molar ratio), were prepared with or without ATRA. ATRA was mixed at the molar ratio of 1:100 of the total lipid content of the liposomes. In the cellular association experiments, liposomes were labeled with a tracer amount of [^{3}H]ATRA. Briefly, the mixture, with or without [^{3}H]ATRA, was first dissolved in chloroform. After vacuum drying and desiccation, pH 7.4 phosphate-buffered saline (−) (PBS (−)) was added for hydration. The preparation was sonicated and passed through a 0.45-μm filter for sterilization.

2.4. Characterization of liposomes

The lipid content of the liposomes was determined by a cholesterol E-test Wako kit (Wako Pure Chemicals Industry, Ltd., Osaka, Japan). The liposomal loading of ATRA was estimated by absorbance at 340 nm after dissolving ATRA incorporated in liposomes in ethanol since the ATRA alone is soluble in ethanol. The zeta potentials of liposomes were measured in 150 mM sodium chloride (NaCl) (pH 7.0) with a laser electrophoresis zeta potential analyzer (LEZA-700, Otsuka Electronics Co., Ltd., Osaka, Japan). The particle sizes of the liposomes were measured in 150 mM NaCl using dynamic light scattering (DLS-7000, Otsuka Electronics Co., Ltd., Osaka, Japan).

2.5. Evaluation of ATRA incorporated in liposomes

The methods used to determine the incorporation ratio of ATRA in liposomes were as described for the liposomal studies [23,24]. Briefly, the [^{3}H]ATRA-incorporated liposomes were ultrafiltered using a micropartition system (Sartorion VIVASPIN 2 ml concentrator 5000 MWCO PES; Vivascience AG, Hannover, Germany) at 1500 × *g* for 15 min. The concentration based on the radioactivity in the preparation (C_T) and in the ultrafiltrate (C_W) was assayed by scintillation counting. The equation for the incorporation ratio in the liposomes was as follows:

$$\text{Incorporation ratio (\%)} = ((C_T - C_W)/C_T) \times 100.$$

2.6. Cellular association study

The cellular association study was performed by the method described previously [25,26]. The A549 cells were plated on a 12-well cluster dish at a density of 5×10^4 cells/3.8 cm^2. Twenty-four hours later, the cells were washed with 1.0 ml PBS (−) and incubated with 1.0 ml medium containing

[^{3}H]ATRA (1% DMSO) or [^{3}H]ATRA incorporated in DSPC/cholesterol or DOTAP/cholesterol liposomes (1 μM ATRA) at 37 or 4 °C. After incubation, the cells were washed thoroughly with Hank's buffered salt solution (HBSS) 5× and solubilized with 1.0 ml 0.3 M NaOH with 0.1% Triton X-100. Aliquots were taken to determine the radioactivity, using a liquid scintillation counter (LSA-500, Beckman Coulter, Inc., Fullerton, CA, USA), and the protein content. The radioactivity data were normalized with respect to the protein contents of the cells.

2.7. Cytotoxicity study

3-(4,5-Dimethyl-2-thiazolyl)-2,5-diphenyl-2*H* tetrazolium bromide (MTT) assay was performed by the method described previously [25,27]. The A549 cells were plated on a 96-well cluster dish at a density of 1×10^4 cells/0.28 cm^2. Twenty-four hours later, the medium containing various concentrations of ATRA, bare liposomes, or ATRA incorporated in liposomes was added to the plates. After 48 h of incubation, the medium was removed and 5 mg/ml MTT solution was added to each well. Cells were incubated for 4 h at 37 °C in 5% CO_2 and then 10% sodium dodecyl sulfate (SDS) solution was added followed by incubation overnight to dissolve formazan crystals. The absorbance was measured at wavelengths of 570 nm in a microplate photometer (Bio-Rad Model 550, Bio-Rad Laboratories, Inc., Hercules, CA, USA).

2.8. DNA fragmentation study

The A549 cells were plated on a 6-well cluster dish at a density of 1×10^5 cells/10.5 cm^2. Twenty-four hours later, the medium containing 1.0 μM ATRA (1% DMSO), bare liposomes, or ATRA incorporated in liposomes was added to the plates. After 48 h of incubation, the supernatant cells and adherent cells were collected. After centrifugation, the pellets were resuspended in 0.2 ml PBS (−). These cells were incubated with 10 μl proteinase K (10 mg/ml), 66.6 μl RNase A (1.5 mg/ml) and 10 μl 10% SDS solution for 30 min at 37 °C, and then incubated with 300 μl NaI solution (6 M NaI, 13 mM EDTA, 0.5% sodium-*N*-lauroylsarcosinate, and 26 mM Tris–HCl, pH 8.0) for 15 min at 60 °C. This was followed by the addition of 500 μl isopropanol and centrifugation at 20,000×*g* for 30 min to extract the total DNA. After agarose electrophoresis at 100 V for 25 min and labeling with ethidium bromide, total DNA was visualized by UV.

2.9. Measurement of cell apoptosis

The A549 cells were plated on a 6-well cluster dish at a density of 1×10^5 cells/10.5 cm^2. Twenty-four hours later, the medium containing 1.0 μM ATRA (1% DMSO), bare liposomes, or ATRA incorporated in liposomes was added to the plates. After 48 h of incubation, cells were trypsonized, collected and centrifuged. After washing in phosphate-buffered saline, 100 μl HEPES buffer including 10 μl annexin V-fluorecsein and 10 μl propidium iodide (PI) were added and cells were resuspended. Labeled cells were counted by flow cytometry (Becton Dickinson Co., Inc., Franklin Lakes, NJ, USA). Annexin V-FITC labeling was measured at 518 nm on the FL1-channel (FITC-detector) and PI staining at 620 nm on the FL2-channel (phycoerytrin-detector).

2.10. Quantification of TIG3 mRNA

The A549 cells were plated on a 6-well cluster dish at a density of 1×10^5 cells/10.5 cm^2. Twenty-four hours later, medium containing 1.0 μM ATRA (1% DMSO) or ATRA incorporated in liposomes was added to the plates. After 48 h incubation, total RNA was extracted using a MagExtractor-RNA kit and MagExtractor System (Toyobo Co., Ltd., Osaka, Japan). The total RNA was subjected to reverse transcription, which was performed by reverse transcription using an RT–PCR core kit (Takara Bio Inc., Shiga, Japan) according to the manufacturer's instructions. Real-time RT–PCR was performed with a LightCycler® 350S system (Roche Diagnostics GmbH, Mannheim, Germany) in LightCycler capillaries using a commercially available master mix containing SYBR–Green I [28]. After the addition of the primers (final concentration=0.2 μM) and the template DNA to the master mix, 30 cycles of denaturation (94 °C for 1 s), annealing (58 °C for 10 s) and extension (72 °C for 10 s) were performed. After the completion of PCR amplification, a melting curve analysis was performed. Primers were designed by the Nihon Gene Research Laboratories, Inc. (Miyagi, Japan). The sequences for tazarotene-induced gene 3 (TIG3) primers were as follows: 5′–ACCATGAGTAC-CAACCACG–3′ and 5′–CCACACCGACTTCAACCTT–3′. The primers produce a PCR fragment of 177 bp. The quality of RNA and cDNA synthesis was determined by amplification of the glyceraldehyde phosphate dehydrogenase (GAPDH) gene as the internal control. The primer sequences for the GAPDH primers were as follows: 5′–TGAACGGGAAGCTCACTGG–3′ and 5′–TCCACCACCCTGTTGCTGTA–3′. The primers produced a PCR fragment of 307 bp.

2.11. Statistical analysis

Statistical comparisons were performed by Student's *t*-test for two groups, and one-way ANOVA for multiple groups. $P<0.05$ was considered indicative of statistical significance.

3. Results

3.1. Physicochemical properties of liposomes

The zeta potentials and the particle sizes of the liposomes are shown in Table 1. The zeta potentials of ATRA incorporated in DOTAP/cholesterol or DSPC/cholesterol liposomes were about +50 and −3 mV indicating that DOTAP/cholesterol or DSPC/cholesterol liposomes are cationic and neutral liposomes. The particle sizes of ATRA incorporated in DOTAP/cholesterol or DSPC/cholesterol liposomes were about 125 and 110 nm. The zeta potentials and particle sizes of DOTAP/cholesterol or DSPC/cholesterol liposomes without

Table 1
The zeta potential and mean particle size of ATRA incorporated in DSPC/cholesterol or DOTAP/cholesterol liposomes

Formulations	Zeta potential (mV)	Particle size (nm)
ATRA incorporated in DOTAP/cholesterol liposomes	51.2±0.80	132±57.3
ATRA incorporated in DSPC/cholesterol liposomes	−3.11±0.30	115±40.0

Each value represent the mean±S.D. of at least three experiments.

ATRA were the same as those of ATRA incorporated in DOTAP/cholesterol or DSPC/cholesterol liposomes [20,29].

3.2. ATRA incorporation of liposomes

The incorporation ratio of ATRA in neutral liposomes and DOTAP/cholesterol liposomes was 95.6±0.42% (n=3) and 97.5±0.38% (n=3), indicating that most of the ATRA was tightly incorporated in DSPC/cholesterol liposomes and DOTAP/cholesterol liposomes.

3.3. Cytotoxic effects of ATRA or ATRA incorporated in liposomes

In the present study, DOTAP/cholesterol and ATRA were mixed at a molar ratio of 100:1. To assess the anti-tumor activity in terms of A549 cells, the cytotoxic effects were examined by MTT assay. In a preliminary experiment, the cytotoxicity of bare DOTAP/cholesterol liposomes was evaluated by varying the concentration of bare cationic liposomes. Higher cytotoxicity was observed in a concentration-dependent manner for DOTAP/cholesterol liposomes; however, no significant cytotoxicity was observed at a concentration of 100 μM bare DOTAP/cholesterol liposomes (data not shown). In the following experiments, therefore, the concentrations of DOTAP/cholesterol liposomes and ATRA for the application to cells were adjusted to 100 and 1.0 μM, respectively, to minimize the cytotoxic effects of DOTAP/cholesterol liposomes.

After application of free ATRA to A549 cells, cytotoxic effects were observed in a concentration-dependent manner (Fig. 1A). In order to examine whether the cytotoxic effects could be enhanced by incorporation into each of the liposomes, ATRA was incorporated into neutral liposomes or DOTAP/cholesterol liposomes. Although ATRA and ATRA incorporated in neutral liposomes did not induce cytotoxicity, a significantly higher cytotoxicity was induced in ATRA incorporated in DOTAP/cholesterol liposomes at an ATRA concentration of 1.0 μM (Fig. 1B).

3.4. Cellular uptake study of ATRA or ATRA incorporated in liposomes

At 37 °C, ATRA uptake was enhanced by incorporation into liposomes, especially in DOTAP/cholesterol liposomes (Fig. 2A). At 4 °C, on the other hand, little uptake of [^{3}H] ATRA was observed and there was no significantly difference among these formulations until 6 h (Fig. 2B).

3.5. Quantitative PCR analysis of TIG3 mRNA of ATRA or ATRA incorporated in liposomes

Fig. 3 shows the effect of the liposomal formulations on the induction of TIG3 mRNA at an ATRA concentration of 1.0 μM. After application of free ATRA, ATRA incorporated in DSPC/cholesterol liposomes, and bare DOTAP/cholesterol liposomal formulations, TIG3 mRNA did not differ significantly from the control (no treatment). However, a significantly higher expression of TIG3 mRNA was observed when ATRA was incorporated into DOTAP/cholesterol liposomes.

3.6. Apoptosis induction of ATRA or ATRA incorporated in liposomes

To study whether 1.0 μM ATRA incorporated in DOTAP/cholesterol liposomes could induce apoptosis, this was

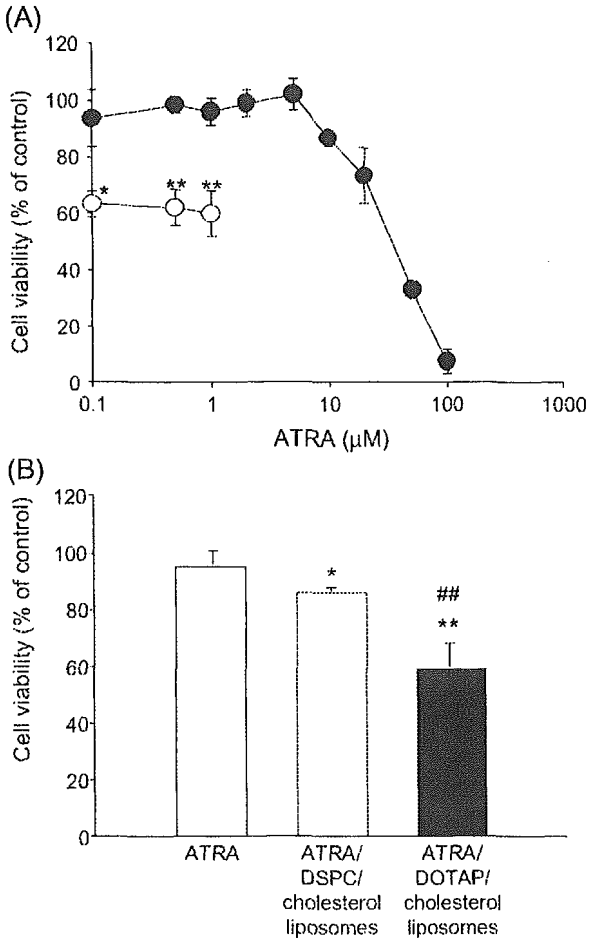

Fig. 1. (A) Cell viability after application of ATRA (●) and ATRA incorporated in DOTAP/cholesterol liposomes (○) at various concentrations for 48 h in A549 cells. Each value represents the mean±S.D. of four experiments. (B) Cell viability after application of 1.0 μM ATRA, ATRA incorporated in DSPC/cholesterol liposomes, or DOTAP/cholesterol liposomes at an ATRA concentration of 1.0 μM for 48 h in A549 cells. Cell viability was determined by MTT assay. Each value represents the mean±S.D. of four experiments. Significant difference $^*P<0.05$ and $^{**}P<0.01$ vs. ATRA, $^{\#\#}P<0.01$ vs. DSPC/cholesterol liposomes.

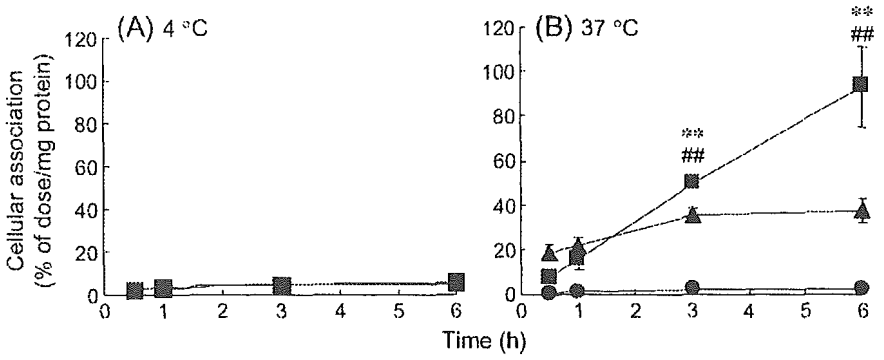

Fig. 2. Cellular association time courses of [^{3}H]ATRA (●), [^{3}H]ATRA incorporated in DSPC/cholesterol liposomes (▲), or DOTAP/cholesterol liposomes (■) at 4 °C (A) and 37 °C (B) in A549 cells. The ATRA concentration was 1.0 μM. Each value represents the mean±S.D. of four experiments. Significant difference $^{\#\#}P<0.01$ vs. ATRA, $^{**}P<0.01$ vs. ATRA incorporated in DSPC/cholesterol liposomes.

examined by flow cytometric analysis and DNA fragment extraction. H_2O_2 was treated as a positive control for apoptosis [30]. Flow cytometric analysis demonstrated that phosphatidylcholine-exposing cells was significantly increased by ATRA incorporated in DOTAP/cholesterol liposomes (27.5±1.80%) compared with free ATRA liposomes (7.66±5.14%), and bare DOTAP/cholesterol liposomal (6.62±5.43%) formulations (Figs. 4 and 5).

Fig. 6 shows the analysis of DNA extracted from A549 cells after application of free ATRA, ATRA incorporated in DSPC/cholesterol liposomes, ATRA incorporated in DOTAP/cholesterol liposomes, and bare liposomal formulations. It was found that giant DNA fragments accumulated in the nucleus of cells treated with ATRA incorporated in cationic liposomes. These results indicate that apoptosis could be efficiently induced by ATRA incorporated in cationic liposome in A549 cells.

4. Discussion

The mean particle sizes of ATRA incorporated DOTAP/cholesterol and DSPC/cholesterol liposomes were about 125 and 110 nm, respectively. On the other hand, the zeta potentials of ATRA-incorporated DOTAP/cholesterol and DSPC/cholesterol liposomes were +50 and −3 mV, respectively. Since the mean particle sizes of these two liposomes were almost identical, the effect of the liposomal charge on ATRA action could be analyzed.

To investigate the cellular uptake mechanisms of ATRA in A549 cells, the cellular association was analyzed at 4 and 37 °C using [^{3}H] ATRA. At 37 °C, ATRA uptake was enhanced by incorporation into liposomes, especially in DOTAP/cholesterol liposomes (Fig. 2A). At 4 °C, ATRA uptake of both liposomes was significantly lower than at 37 °C (Fig. 2B). These results suggested that ATRA is efficiently taken up by

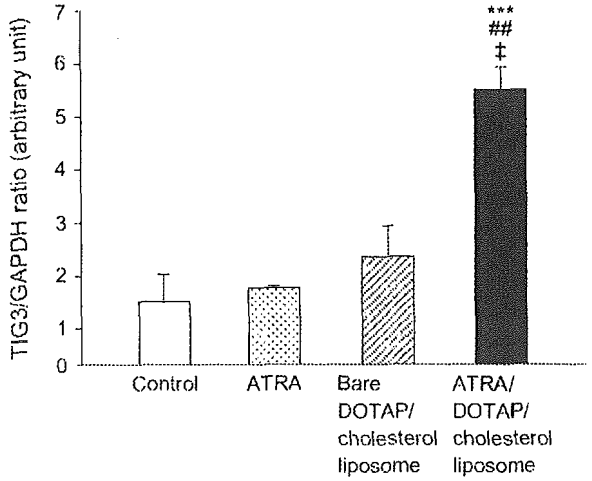

Fig. 3. Quantitative PCR analysis of TIG3 mRNA levels in A549 cells. Cells were incubated with 1.0 μM ATRA, bare DOTAP/cholesterol liposomes, or ATRA incorporated in DOTAP/cholesterol liposomes for 48 h in A549 cells. As a control, the cells were incubated with 1% DMSO. The results are expressed as arbitrary units of the TIG3 level divided by the GAPDH level. Each value represents the mean±S.D. of four experiments. Significant difference $^{***}P<0.001$ vs. (1% DMSO), $^{\#\#}P<0.01$ vs. ATRA, and $^{\ddagger}P<0.05$ vs. bare DOTAP/cholesterol liposomes.

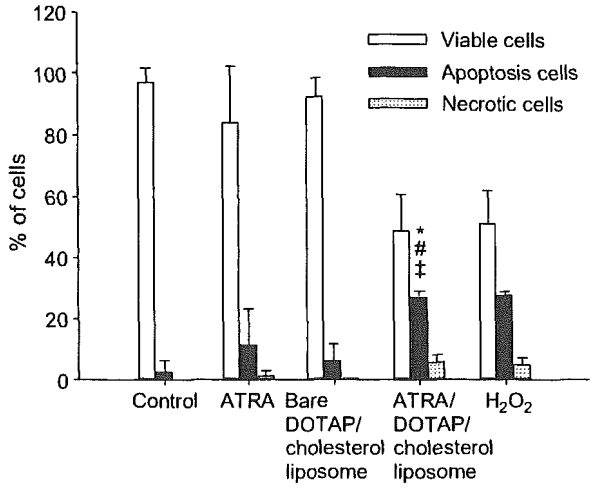

Fig. 4. Flow cytometric analysis of A549 cells treated with 1.0 μM ATRA, bare DOTAP/cholesterol liposomes, or ATRA incorporated in DOTAP/cholesterol liposomes for 48 h in A549 cells. After treatment, the cells were stained with annexin V-fluorescein and PI. As a control, cells were incubated with 1% DMSO and 400 μM H_2O_2. Each value represents the mean±S.D. of four experiments. Significant difference $^{*}P<0.05$ vs. control (1% DMSO), $^{\#}P<0.05$ vs. ATRA, and $^{\ddagger}P<0.05$ vs. bare DOTAP/cholesterol liposomes.

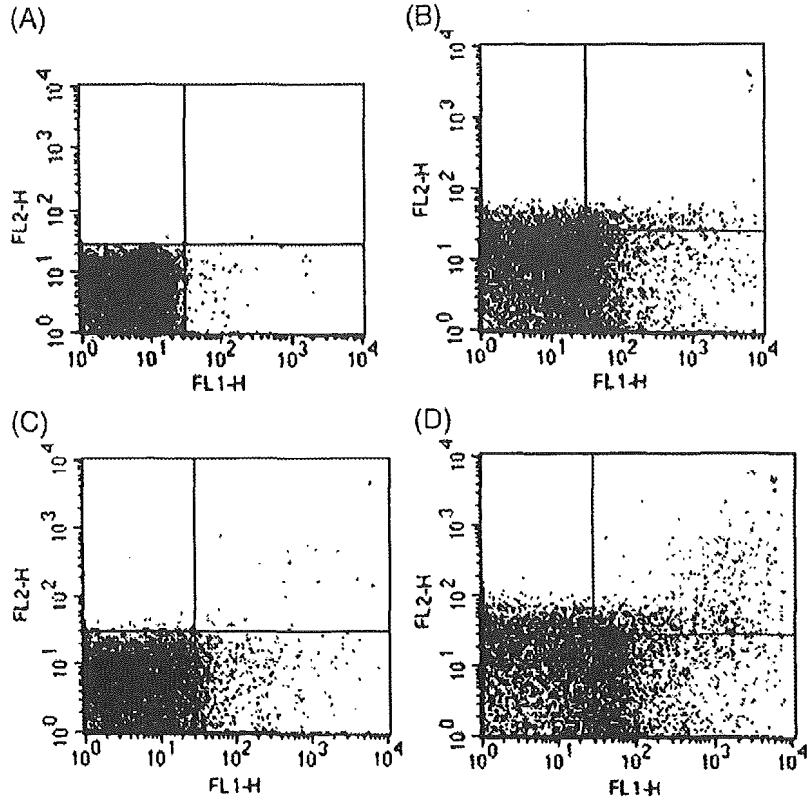

Fig. 5. Typical flow cytometric analysis of A549 cells treated without (A) or with 1.0 μM ATRA (B), bare DOTAP/cholesterol liposomes (C), or ATRA incorporated in DOTAP/cholesterol liposomes (D) for 48 h in A549 cells.

endocytosis when it is incorporated in DOTAP/cholesterol liposomes in A549 cells. This uptake mechanism agrees with the results of the uptake of plasmid DNA complexed with cationic liposomes [31–33]. The cellular association difference between 37 and 4 °C reflects the amount of ATRA internalized in the A549 cells. As far as the types of liposome formulations are concerned, the internalized ATRA by ATRA incorporated in DOTAP/cholesterol liposomes was much higher than that in DSPC/cholesterol liposomes (Fig. 2A and B). Since ATRA incorporated in DOTAP/cholesterol liposomes had positive surface charge (Table 1), they could interact with the cellular membrane, which possesses a negative charge, through electrostatic interaction, and be effectively internalized into the cells.

In order to evaluate whether cytotoxicity was enhanced by ATRA incorporated in DOTAP/cholesterol liposomes, MTT assay was performed. Recently, Manna and Aggarwal [15] and Higuchi et al. [12] reported that no growth inhibitory effect in

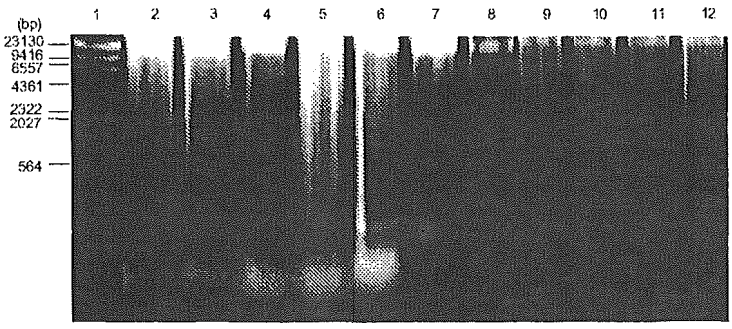

Fig. 6. Agarose gel electrophoresis of DNA extracted from A549 cells incubated with 1.0 μM ATRA, ATRA incorporated in DOTAP/cholesterol or DSPC/cholesterol liposomes and bare DOTAP/cholesterol or bare DSPC/cholesterol liposomes for 48 h in A549 cells. Lane 1: DNA marker. Lanes 2–4: DNA from cells treated with ATRA at ATRA concentrations of 0.5, 1.0, and 50 μM, respectively. Lanes 5–6: DNA from cells treated with ATRA incorporated in DOTAP/cholesterol liposomes at ATRA concentrations of 0.5 and 1.0 μM. Lanes 7–8: DNA from cells treated with DOTAP/cholesterol liposomes at total lipid concentrations of 59 and 117 μM. Lanes 9–10: DNA from cells treated with ATRA incorporated in DSPC/cholesterol liposomes at ATRA concentrations of 0.5 and 1 μM. Lanes 11–12: DNA from cells treated with DSPC/cholesterol liposomes at total lipid concentrations of 27 and 55 μM. DNA was extracted from about 5×10^5 cells and loaded in each well.

A549 cells was observed at ATRA concentrations of 2.0 and 1.0 μM, although the growth of other ATRA sensitive cell lines was inhibited at these concentrations. We also observed a similar result showing that there was no cytotoxic effect below 10 μM free ATRA (Fig. 1A), indicating that A549 cells are ATRA-insensitive (resistant). In the present study, we demonstrated that when ATRA was incorporated in cationic liposomes composed of DOTAP/cholesterol, a potent cytotoxic effect was exhibited even at 0.1, 0.5, and 1.0 μM (Fig. 1B), indicating that the cytotoxicity in A549 cells can be efficiently induced by ATRA incorporated in DOTAP/cholesterol liposomes. These cytotoxicity results support our hypothesis that intracellular delivery of ATRA should be able to overcome ATRA resistance in A549 cells.

To investigate whether ATRA incorporated in DOTAP/cholesterol liposomes could induce apoptosis, flow cytometric analysis and extraction of DNA fragments were performed. The flow cytometric analysis demonstrated that phosphatidylcholine-exposing cells were significantly increased by ATRA incorporated in DOTAP/cholesterol liposomes compared with free ATRA, and ATRA incorporated in DSPC/cholesterol liposomes (Figs. 4 and 5). Furthermore, the giant DNA fragments accumulated in the nucleus of cells treated with ATRA incorporated in cationic liposomes (Fig. 6). These findings strongly suggest that apoptosis can be induced by ATRA incorporated DOTAP/cholesterol liposomes in A549 cells.

The TIG3 gene is a retinoic acid inducible class II tumor suppressor gene down-regulated in several human tumors and malignant cell lines [34]. To explore the mechanism of cytotoxicity and induction of apoptosis by ATRA incorporated in DOTAP/cholesterol liposomes, we examined the expression of mRNA of TIG3. TIG3 mRNA was not induced by free ATRA in A549 cells at an ATRA concentration of 1.0 μM. This observation agrees with the results reported by Higuchi et al. [12]. On the other hand, we showed that the amount of TIG3 mRNA increased in A549 cells treated with ATRA (1.0 μM) incorporated in DOTAP/cholesterol liposomes in A549 cells. In addition, the induction of TIG3 mRNA (Fig. 3) is in agreement with the cytotoxicity (Fig. 1) and apoptosis (Figs. 4–6) results. These observations provide evidence that TIG3 induction by ATRA incorporated in DOTAP/cholesterol liposomes induces cytotoxicity and/or apoptosis in A549 cells.

Higuchi et al. also reported that ATRA-induced TIG3 expression takes place through the nuclear retinoid pathway [12]. As shown in Fig. 2, we demonstrated that ATRA were efficiently internalized in cells by incorporation into DOTAP/cholesterol liposomes and this phenomenon corresponds to the expression of TIG3 mRNA (Fig. 3). Therefore, these observations lead us to believe that ATRA is efficiently delivered to the nucleus by incorporation into DOTAP/cholesterol liposomes.

Recently, much effort has been devoted to the development of cationic liposome-mediated gene delivery systems due to their favorable characteristics. Since pDNA complexed with cationic liposomes (i.e. lipoplexes) accumulate in the lung immediately after intravenous administration [35], they lead to a high gene expression in that tissue [36–39]. Recently, we have reported that intravenously injected interferon encoding plasmid DNA complexed with cationic liposomes prevents lung metastases in a mouse lung CT26 metastasis model [40]. Since ATRA are incorporated in liposomal lipid membranes, ATRA are able to be introduced into the cytokine gene therapy system without the inhibition of the lipoplex formation via electrostatic interaction. Thus, the combination of cytokine therapy and differentiation therapy might be used to improve the treatment of NSCLC in the near future.

In conclusion, we have demonstrated that ATRA incorporated in cationic liposomes composed of DOTAP/cholesterol are efficiently internalized into A549 cells, producing potent cytotoxic and apoptosis-inducing effects on ATRA-insensitive (resistant) A549 cells. The enhanced expression of TIG3 mRNA tumor suppressor gene by ATRA incorporation into DOTAP/cholesterol liposomes might partly explain the mechanism of enhanced cytotoxicity and/or apoptosis in A549 cells. These observations provide valuable information to help in the design of differentiation therapy by ATRA in NSCLC.

Acknowledgements

This work was supported in part by Grant-in-Aids for Scientific Research from the Ministry of Education, Culture, Sports, Science, and Technology of Japan, and by Health and Labour Sciences Research Grants for Research on Advanced Medical Technology from the Ministry of Health, Labour and Welfare of Japan.

References

[1] A.I. Spira, M.A. Carducci, Differentiation therapy, Curr. Opin. Pharmacol. 3 (2003) 338–343.
[2] M.E. Huang, Y.C. Ye, S.R. Chen, J.R. Chai, J.X. Lu, L. Zhoa, L.J. Gu, Z.Y. Wang, Use of all-*trans* retinoic acid in the treatment of acute promyelocytic leukemia, Blood 72 (1988) 567–572.
[3] S. Castaigne, C. Chomienne, M.T. Daniel, P. Ballerini, R. Berger, P. Fenaux, L. Degos, All-*trans* retinoic acid as a differentiation therapy for acute promyelocytic leukemia: I. Clinical results, Blood 76 (1990) 1704–1709.
[4] D.G. Kim, B.H. Jo, K.R. You, D.S. Ahn, Apoptosis induced by retinoic acid in Hep3B cells in vitro, Cancer Lett. 107 (1996) 149–159.
[5] K. Hayashi, H. Yokozaki, K. Naka, W. Yasui, R. Lotan, E. Tahara, Overexpression of retinoic acid receptor β induces growth arrest and apoptosis in oral cancer cells, Jpn. J. Cancer Res. 92 (2001) 42–50.
[6] Y. Choi, S.Y. Kim, S.H. Kim, J. Yang, K. Park, Y. Byun, Inhibition of tumor growth by biodegradable microspheres containing all-*trans*-retinoic acid in a human head-and-neck cancer xenograft, Int. J. Cancer 107 (2003) 145–148.
[7] Y.F. Lee, B.Y. Bao, C. Chang, Modulation of the retinoic acid-induced cell apoptosis and differentiation by the human TR4 orphan nuclear receptor, Biochem. Biophys. Res. Commun. 323 (2004) 876–883.
[8] C. Di, S. Liao, D.C. Adamson, T.J. Parrett, D.K. Broderick, Q. Shi, C. Lengauer, J.M. Cummins, V.E. Velculescu, D.W. Fults, R.E. McLendon, D.D. Bigner, H. Yan, Identification of OTX2 as a medulloblastoma oncogene whose product can be targeted by all-*trans* retinoic acid, Cancer Res. 65 (2005) 919–924.
[9] S.J. Freemantle, M.J. Spinella, E. Dmitrovsky, Retinoids in cancer therapy and chemoprevention: promise meets resistance, Oncogene 22 (2003) 7305–7315.

[10] D. DiSepio, C. Ghosn, R.L. Eckert, A. Deucher, N. Robinson, M. Duvic, R.A. Chandraratna, S. Nagpal, Identification and characterization of a retinoid-induced class II tumor suppressor/growth regulatory gene, Proc. Natl. Acad. Sci. U. S. A. 95 (1998) 14811–14815.

[11] A. Deucher, S. Nagpal, R.A. Chandraratna, D. DiSepio, N.A. Robinson, S.R. Dashti, R.L. Eckert, The carboxy-terminal hydrophobic domain of TIG3, a class II tumor suppressor protein, is required for appropriate cellular localization and optimal biological activity, Int. J. Oncol. 17 (2000) 1195–1203.

[12] E. Higuchi, R.A. Chandraratna, W.K. Hong, R. Lotan, Induction of TIG3, a putative class II tumor suppressor gene, by retinoic acid in head and neck and lung carcinoma cells and its association with suppression of the transformed phenotype, Oncogene 22 (2003) 4627–4635.

[13] J. Geradts, J.Y. Chen, E.K. Russell, J.R. Yankaskas, L. Nieves, J.D. Minna, Human lung cancer cell lines exhibit resistance to retinoic acid treatment, Cell Growth Differ. 4 (1993) 799–809.

[14] B.M. van der Leede, C.E. van den Brink, P.T. van der Saag, Retinoic acid receptor and retinoid X receptor expression in retinoic acid-resistant human tumor cell lines, Mol. Carcinog. 8 (1993) 112–122.

[15] S.K. Manna, B.B. Aggarwal, All-*trans*-retinoic acid upregulates TNF receptors and potentiates TNF-induced activation of nuclear factors-κB, activated protein-1 and apoptosis in human lung cancer cells, Oncogene 19 (2000) 2110–2119.

[16] C.A. Lipinski, F. Lombardo, B.W. Dominy, P.J. Feeney, Experimental and computational approaches to estimate solubility and permeability in drug discovery and development settings, Adv. Drug Delivery Rev. 46 (2001) 3–26.

[17] S. Kawakami, P. Opanasopit, M. Yokoyama, N. Chansri, T. Yamamoto, T. Okano, F. Yamashita, M. Hashida, Biodistribution characteristics of all-*trans* retinoic acid incorporated in liposomes and polymeric micelles following intravenous administration, J. Pharm. Sci. 94 (2005) 2606–2615.

[18] G. Thurston, J.W. McLean, M. Rizen, P. Baluk, A. Haskell, T.J. Murphy, D. Hanahan, D.M. McDonald, Cationic liposomes target angiogenic endothelial cells in tumors and chronic inflammation in mice, J. Clin. Invest. 101 (1998) 1401–1413.

[19] S. Krasnici, A. Werner, M.E. Eichhorn, M. Schmitt-Sody, S.A. Pahernik, B. Sauer, B. Schulze, M. Teifel, U. Michaelis, K. Naujoks, M. Dellian, Effect of the surface charge of liposomes on their uptake by angiogenic tumor vessels, Int. J. Cancer 105 (2003) 561–567.

[20] W. Yeeprae, S. Kawakami, F. Yamashita, M. Hashida, Physicochemical and pharmacokinetic characteristics of cationic liposomes, Pharmazie (in press).

[21] S. Kawakami, J. Wong, A. Sato, Y. Hattori, F. Yamashita, M. Hashida, Biodistribution characteristics of mannosylated, fucosylated, and galactosylated liposomes in mice, Biochim. Biophys. Acta 1524 (2000) 258–265.

[22] S. Kawakami, C. Munakata, S. Fumoto, F. Yamashita, M. Hashida, Novel galactosylated liposomes for hepatocyte-selective targeting of lipophilic drugs, J. Pharm. Sci. 90 (2001) 105–113.

[23] S. Kawakami, K. Yamamura, T. Mukai, K. Nishida, J. Nakamura, T. Sakaeda, M. Nakashima, H. Sasaki, Sustained ocular delivery of tilisolol to rabbits after topical administration or intravitreal injection of lipophilic prodrug incorporated in liposomes, J. Pharm. Pharmacol. 53 (2001) 1157–1161.

[24] M. Teshima, S. Kawakami, K. Nishida, J. Nakamura, T. Sakaeda, H. Terazono, T. Kitahara, M. Nakashima, H. Sasaki, Prednisolone retention in integrated liposomes by chemical approach and pharmaceutical approach, J. Controlled Release 97 (2004) 211–218.

[25] S. Kawakami, F. Yamashita, M. Nishikawa, Y. Takakura, M. Hashida, Asialoglycoprotein receptor-mediated gene transfer using novel galactosylated cationic liposomes, Biochem. Biophys. Res. Commun. 252 (1998) 78–83.

[26] P. Opanasopit, Y. Higuchi, S. Kawakami, F. Yamashita, M. Nishikawa, M. Hashida, Involvement of serum mannan binding proteins and mannose receptors in uptake of mannosylated liposomes by macrophages, Biochim. Biophys. Acta 1511 (2001) 134–145.

[27] S. Kawakami, A. Sato, M. Nishikawa, F. Yamashita, M. Hashida, Mannose receptor-mediated gene transfer into macrophages using novel mannosylated cationic liposomes, Gene Ther. 7 (2000) 292–299.

[28] Y. Hattori, S. Kawakami, S. Suzuki, F. Yamashita, M. Hashida, Enhancement of immune responses by DNA vaccination through targeted gene delivery using mannosylated cationic liposome formulations following intravenous administration in mice, Biochem. Biophys. Res. Commun. 317 (2004) 992–999.

[29] C. Managit, S. Kawakami, F. Yamashita, M. Hashida, Effect of galactose density on asialoglycoprotein receptor-mediated uptake of galactosylated liposomes, J. Pharm. Sci. 94 (2005) 2266–2275.

[30] T. Geiser, M. Ishigaki, C. van Leer, M.A. Matthay, V.C. Broaddus, H_2O_2 inhibits alveolar epithelial wound repair in vitro by induction of apoptosis, Am. J. Physiol.: Lung Cell. Mol. Physiol. 287 (2004) L448–L453.

[31] F. Sakurai, R. Inoue, Y. Nishino, A. Okuda, O. Matsumoto, T. Taga, F. Yamashita, Y. Takakura, M. Hashida, Effect of DNA/liposome mixing ratio on the physicochemical characteristics, cellular uptake and intracellular trafficking of plasmid DNA/cationic liposome complexes and subsequent gene expression, J. Controlled Release 66 (2000) 255–269.

[32] D. Lleres, J.M. Weibel, D. Heissler, G. Zuber, G. Duportail, Y. Mely, Dependence of the cellular internalization and transfection efficiency on the structure and physicochemical properties of cationic detergent/DNA/liposomes, J. Gene Med. 6 (2004) 415–428.

[33] C.M. Wiethoff, J.G. Koe, G.S. Koe, C.R. Middaugh, Compositional effects of cationic lipid/DNA delivery systems on transgene expression in cell culture, J. Pharm. Sci. 93 (2004) 108–123.

[34] K. Lotz, T. Kellner, M. Heitmann, I. Nazarenko, A. Noske, A. Malek, A. Gontarewicz, R. Schafer, C. Sers, Suppression of the TIG3 tumor suppressor gene in human ovarian carcinomas is mediated via mitogen-activated kinase-dependent and -independent mechanisms, Int. J. Cancer 116 (2005) 894–902.

[35] S. Kawakami, F. Yamashita, K. Nishida, J. Nakamura, M. Hashida, Glycosylated cationic liposomes for cell-selective gene delivery, Crit. Rev. Ther. Drug Carrier Syst. 19 (2002) 171–190.

[36] N. Zhu, D. Liggitt, Y. Liu, R. Debs, Systemic gene expression after intravenous DNA delivery into adult mice, Science 261 (1993) 209–211.

[37] S. Li, L. Huang, In vivo gene transfer via intravenous administration of cationic lipid–protamine–DNA (LPD) complexes, Gene Ther. 4 (1997) 891–900.

[38] S. Kawakami, S. Fumoto, M. Nishikawa, F. Yamashita, M. Hashida, In vivo gene delivery to the liver using novel galactosylated cationic liposomes, Pharm. Res. 17 (2000) 306–313.

[39] S. Kawakami, A. Sato, M. Yamada, F. Yamashita, M. Hashida, The effect of lipid composition on receptor-mediated in vivo gene transfection using mannosylated cationic liposomes in mice, STP Pharm. Sci. 11 (2001) 117–120.

[40] F. Sakurai, T. Terada, M. Maruyama, Y. Watanabe, F. Yamashita, Y. Takakura, M. Hashida, Therapeutic effect of intravenous delivery of lipoplexes containing the interferon-β gene and poly I: poly C in a murine lung metastasis model, Cancer Gene Ther. 10 (2003) 661–668.

0022-3565/05/3152-484–493$20.00
THE JOURNAL OF PHARMACOLOGY AND EXPERIMENTAL THERAPEUTICS
Copyright © 2005 by The American Society for Pharmacology and Experimental Therapeutics
JPET 315:484–493, 2005

Vol. 315, No. 2
89516/3054856
Printed in U.S.A.

Interaction with Blood Components Plays a Crucial Role in Asialoglycoprotein Receptor-Mediated in Vivo Gene Transfer by Galactosylated Lipoplex

Shintaro Fumoto, Shigeru Kawakami, Kosuke Shigeta, Yuriko Higuchi, Fumiyoshi Yamashita, and Mitsuru Hashida

Department of Drug Delivery Research, Graduate School of Pharmaceutical Sciences, Kyoto University, Kyoto, Japan

Received May 13, 2005; accepted July 19, 2005

ABSTRACT

In this study, we evaluated the effect of blood components (whole blood and serum) on asialoglycoprotein receptor-mediated in vivo gene transfer. The hepatic transfection activity of galactosylated lipoplex preincubated with serum was approximately 10 times higher than that without incubation after intraportal injection in mice. However, preincubation with whole blood significantly reduced hepatic transfection activity. Fluorescent resonance energy transfer analysis and agarose gel electrophoresis revealed that preincubation with serum reduced the degree of destabilization of the galactosylated lipoplex in blood, partially supporting enhanced hepatic transfection activity by preincubation with serum. Inhibition of hepatic transfection activity by predosing galactosylated bovine serum albumin indicated that the galactosylated lipoplex exposed to serum is recognized by asialoglycoprotein-receptors on hepatocytes. Inactivation of serum prior to mixing with galactosylated lipoplex reduced liver accumulation and completely abolished enhancement of hepatic transfection activity by preincubation with active serum, suggesting that not only the stability of the lipoplex in blood but also the serum opsonin activity plays important roles. Alternatively, preincubation with inactivated serum reduced the lung accumulation and inflammatory cytokine production of galactosylated lipoplex. The information provided by this study will be valuable for the future use, design, and development of galactosylated lipoplex for in vivo asialoglycoprotein receptor-mediated gene transfer.

For effective and safe in vivo gene transfer, the development of targeted gene delivery systems is a promising approach. To achieve targeted gene delivery to hepatocytes, galactose has been shown to be a promising targeting ligand to hepatocytes (liver parenchymal cells) because these cells possess a large number of asialoglycoprotein receptors that recognize the galactose units on the glycoproteins or synthetic galactosylated carriers (Kawakami et al., 2002). Recently, we have developed several types of macromolecular and particulate gene carriers for hepatocyte-selective gene transfection in vivo (Kawakami et al., 2000; Fumoto et al., 2003a, 2004; Morimoto et al., 2003). These include galactosylated cationic liposomes containing Gal-C4-Chol, which can be efficiently recognized by asialoglycoprotein receptors in hepatocytes in vivo (Kawakami et al., 2000; Fumoto et al., 2004). However, a number of possible barriers are associated with in vivo gene delivery (Yang and Huang, 1997; Li et al., 1999; Sakurai et al., 2001a; Fumoto et al., 2003b). Detailed information regarding these barriers is needed to allow the rational design of effective gene carriers.

When galactosylated liposome/pDNA complex (lipoplex) was injected into the portal vein of mice, most of it was taken up by the liver (Kawakami et al., 2000). However, the level of in vivo gene expression was not as high as that expected from the in vitro results. Thus, there must be several barriers associated intrinsically with in vivo situations, such as convective blood flow in the liver, passage through the sinusoids,

This work was supported in part by grants-in-aid for Scientific Research from the Ministry of Education, Culture, Sports, Science, and Technology of Japan, by Health and Labor Sciences Research Grants for Research on Hepatitis and Bovine Spongiform Encephalopathy from the Ministry of Health, Labor and Welfare of Japan, by a grant-in-aid from the Mochida Memorial Foundation for Medical and Pharmaceutical Research, and by the 21st Century Center for Excellence Program "Knowledge Information Infrastructure for Genome Science."

Article, publication date, and citation information can be found at http://jpet.aspetjournals.org.

doi:10.1124/jpet.105.089516.

ABBREVIATIONS: Gal-C4-Chol, cholesten-5-yloxy-*N*-(4-((1-imino-2-D-thiogalactosylethyl)amino)butyl)formamide; pDNA, plasmid DNA; DOTMA, *N*-[1-(2,3-dioleyloxy)propyl]-*n*,*n*,*n*-trimethylammonium chloride; Chol, cholesterol; lipoplex, cationic liposome/pDNA complex; Rh-DOPE, 1,2-dioleoyl-*sn*-glycero-3-phosphoethanolamine-*N*-(lissamine rhodamine B sulfonyl); BSA, bovine serum albumin; Gal-BSA, galactosylated BSA; AUC, area under the curve; PC, parenchymal cells; NPC, nonparenchymal cells; IFN-γ, interferon-γ; MRT, mean residence time; FRET, fluorescent resonance energy transfer.

and tissue interactions. To elucidate these barrier processes, we investigated the hepatic disposition profiles of galactosylated lipoplex in rat liver perfusion experiments (Fumoto et al., 2003b), which allowed us to determine the uptake characteristics of a range of substances under different experimental conditions with the structure of the liver remaining intact. In our study, we demonstrated that the penetration of the galactosylated lipoplex through the hepatic fenestrated endothelium to the parenchymal cells was greatly restricted in perfused rat liver (Fumoto et al., 2003b).

It has been reported that lipoplex is able to interact with various types of biological components (e.g., serum proteins) because of their strong positive charge (Mclean et al., 1999; Sakurai et al., 2001b). The presence of serum proteins has been also thought to be a limiting factor for in vitro transfection by lipoplex. Understanding the interaction with the blood cells as well as serum proteins is crucial for the successful development of an effective gene delivery vector. However, the effects of interaction between the galactosylated lipoplex and blood components on asialoglycoprotein receptor-mediated gene transfer have not been well documented. Because the galactosylated lipoplex must pass through the endothelial cell barriers to reach the hepatocytes, the interaction between blood components and galactosylated lipoplex needs to be examined in detail.

In this study, we evaluated the effects of blood components (whole blood and serum) on physicochemical properties, the in situ and in vivo disposition, and the in vivo transfection efficiency of galactosylated lipoplex.

Materials and Methods

Materials. *N*-(4-Aminobutyl)carbamic acid *tert*-butyl ester and DOTMA were obtained from Tokyo Chemical Industry Co. Ltd. (Tokyo, Japan). Chol and Clear-Sol I were obtained from Nacalai Tesque (Kyoto, Japan), and Soluene 350 was purchased from PerkinElmer Life and Analytical Sciences (Boston, MA). Cholesteryl chloroformate and collagenase type IA were obtained from Sigma-Aldrich (St. Louis, MO). Rh-DOPE was purchased from Avanti Polar Lipids (Alabaster, AL). [α-^{32}P]dCTP (3000 Ci/mmol) was obtained from GE Healthcare (Little Chalfont, Buckinghamshire, UK). Galactosylated bovine serum albumin (Gal-BSA) as a ligand of asialoglycoprotein receptors was synthesized as described in our earlier study (Nishikawa et al., 1995). All other chemicals were of the highest purity available.

Animals. Female 5-week-old ICR mice (20–23 g) and male Wistar rats (170–210 g) were purchased from the Shizuoka Agricultural Cooperative Association for Laboratory Animals (Shizuoka, Japan). All animal experiments were carried out in accordance with the Principles of Laboratory Animal Care as adopted and promulgated by the National Institutes of Health (Bethesda, MD) and the Guidelines for Animal Experiments of Kyoto University.

Construction and Preparation of pDNA. pCMV-luciferase was constructed by subcloning the HindIII/XbaI firefly luciferase cDNA fragment from pGL3-control vector (Promega, Madison, WI) into the polylinker of pcDNA3 vector (Invitrogen, Carlsbad, CA). pDNA was amplified in the *Escherichia coli* strain DH5α, isolated, and purified using a QIAGEN Endofree Plasmid Giga Kit (QIAGEN GmbH, Hilden, Germany). Purity was confirmed by 1% agarose gel electrophoresis followed by ethidium bromide staining, and the pDNA concentration was measured by UV absorption at 260 nm. The pDNA for in vivo distribution and in situ liver perfusion experiments was labeled with [α-^{32}P]dCTP by nick translation (Sambrook et al., 1989).

Synthesis of Gal-C4-Chol. Gal-C4-Chol was synthesized as reported previously (Kawakami et al., 1998). In brief, cholesteryl chloroformate and *N*-(4-aminobutyl)carbamic acid *tert*-butyl ester were reacted in chloroform for 24 h at room temperature. A solution of trifluoroacetic acid and chloroform was added dropwise, and the mixture was stirred for 4 h at 4°C. The solvent was evaporated to obtain *N*-(4-aminobutyl)-(cholesten-5-yloxyl)formamide, which was then combined with 2-imino-2-methoxyethyl-1-thiogalactoside, and the mixture was stirred for 24 h at 37°C. After evaporation, the resultant material was suspended in water, dialyzed against distilled water for 48 h (12 kDa cut-off dialysis tubing), and then lyophilized.

Preparation of Galactosylated Cationic Liposomes. Mixtures of DOTMA, Chol, and Gal-C4-Chol were dissolved in chloroform at a molar ratio of 2:1:1 for galactosylated liposomes, vacuum-desiccated, and resuspended in sterile 5% dextrose solution at a concentration of 4 mg of total lipids/ml. The suspension was sonicated for 3 min, and the resulting liposomes were extruded 10 times through double-stacked 100-nm polycarbonate membrane filters.

Preparation of Galactosylated Lipoplex. Four hundred and twenty microliters of 286 μg/ml pDNA in 5% dextrose solution was mixed with an equal volume of galactosylated cationic liposomes at 1657 μg/ml and incubated for 30 min. The mixing ratio of liposomes and pDNA was expressed as a (±)-charge ratio, which is the molar ratio of cationic lipids to pDNA phosphate residues (Yang and Huang, 1997). A charge ratio of unity was obtained with 2.52 μg of total lipid/μg pDNA for galactosylated liposomes in this study. As far as the charge ratio was concerned, we selected a charge ratio of +2.3 for all experiments to obtain the most effective transfection activity for receptor-mediated gene transfer (Kawakami et al., 2000, 2004) and to prevent any effect of free liposomes (Eastman et al., 1997; Sakurai et al., 2001a). The particle size and ζ-potential of the galactosylated lipoplex were measured using a dynamic light-scattering spectrophotometer (LS-900; Otsuka Electronics, Osaka, Japan) and a laser electrophoresis ζ-potential analyzer (LEZA-500T; Otsuka Electronics), respectively.

Preparation of Serum and Whole Blood. Mouse or rat serum was prepared by the method of Sakurai et al. (2001a). In brief, mouse serum was isolated from fresh whole blood obtained from ICR mice. Blood was collected from the vena cava under anesthesia without heparin treatment and allowed to stand for 3 h at 37°C and then overnight at 4°C. Serum was collected after centrifugation. Inactivated serum was prepared by heating serum for 30 min at 56°C. Whole blood was collected in a heparinized syringe from ICR mice. An erythrocyte suspension was prepared as described in a previous report (Senior et al., 1991) by washing whole blood three times with phosphate-buffered saline (pH 7.4).

In Vivo Transfection Experiments. Before intraportal injection, galactosylated lipoplex was incubated with blood components for 5 min at 37°C. Mice were anesthetized by intraperitoneal administration of 50 mg/kg pentobarbital sodium. An incision was made in the abdomen, and the portal vein was exposed. The lipoplex preincubated with blood components was injected into the portal vein at a volume of 15 ml/kg, and the abdomen was closed with wound clips. Liver samples were taken 6 h after injection, and each sample was homogenized with lysis buffer (0.1 M Tris/HCl containing 0.05% Triton X-100 and 2 mM EDTA, pH 7.8). After three cycles of freezing and thawing, the homogenates were centrifuged at 10,000*g* for 10 min at 4°C. Twenty microliters of each supernatant was mixed with 100 μl of luciferase assay solution (Picagene; Toyo Ink Mfg. Co. Ltd., Tokyo, Japan), and the light produced was immediately measured using a luminometer (Lumat LB 9507; Berthold Technologies, Bad Wildbad, Germany). The protein content of the samples was determined using a protein quantification kit (Dojindo Molecular Technologies Inc., Gaithersburg, MD). For evaluation of the intrahepatic localization of gene expression, the luciferase activities in the liver parenchymal (PC) and nonparenchymal cells (NPC) were independently determined after centrifugal separation of PC and NPC in

collagenase-digested liver as previously described (Kawakami et al., 2000). In the inhibition experiments involving hepatic transfection, mice received intravenous injections of 20 mg/kg Gal-BSA 1 min before the intraportal injection of the lipoplex.

In Vivo Distribution Study. ^{32}P-Labeled galactosylated lipoplex preincubated with blood components was injected into the portal vein of mice at a volume of 15 ml/kg. At each collection time point, blood was collected from the vena cava and mice were killed at the end of the experiment. The liver, kidneys, spleen, heart, and lungs were removed, washed with saline, blotted dry, and weighed. Ten microliters blood and a small amount of each tissue were digested with 0.7 ml of Soluene-350 by incubating overnight at 45°C. After digestion, 0.2 ml of isopropanol, 0.2 ml of 30% hydroperoxide, 0.1 ml of 5 M HCl, and 5.0 ml of Clear-Sol I were added. The samples were stored overnight, and the radioactivity was measured in a scintillation counter (LSA-500; Beckman Coulter, Inc., Fullerton, CA).

Calculation of Organ Uptake Clearance. Tissue distribution data were evaluated using organ uptake clearances as reported previously (Takakura et al., 1987). In brief, the tissue uptake rate can be described by the following equation,

$$\frac{dX_t}{dt} = \mathrm{CL_{uptake}} \times \mathrm{C_b} \quad (1)$$

where X_t is the amount of ^{32}P-labeled galactosylated lipoplex in the tissue at time t, $\mathrm{CL_{uptake}}$ is the tissue uptake clearance, and C_b is the blood concentration of ^{32}P-labeled galactosylated lipoplex. Integration of eq. 1 gives the following,

$$X_t = \mathrm{CL_{uptake}} \times \mathrm{AUC_{(0-t)}} \quad (2)$$

where area under the curve $(\mathrm{AUC})_{(0-t)}$ represents the area under the blood concentration time curve from time 0 to t. The $\mathrm{CL_{uptake}}$ value can be obtained from the initial slope of a plot of X_t versus $\mathrm{AUC_{(0-t)}}$.

Liver Perfusion Experiments and Pharmacokinetic Analysis. In situ liver perfusion studies were carried out as reported previously (Nishida et al., 1989; Fumoto et al., 2003b). In brief, the portal vein was catheterized with a polyether nylon catheter (SURFLO i.v. catheter, 16 G'2"; Terumo Co., Tokyo, Japan) and immediately perfused with Krebs-Ringer-bicarbonate buffer supplemented with 10 mM glucose (oxygenated with 95% O_2 and 5% CO_2, adjusted to pH 7.4 at 37°C). The perfusate did not contain serum proteins and blood cells. The perfusate was circulated using a peristaltic pump (SJ-1211; Atto Bioscience, Tokyo, Japan) at a flow rate of 13 ml/min. After a stabilization period of 25 min, ^{32}P-labeled galactosylated lipoplex preincubated with rat serum or whole blood (30 μg of pDNA/300 μl) was administered via the portal vein using a six-position rotary valve injector (Type 50 Teflon rotary valves; Rheodyne Inc., Cotati, CA). After the addition of 5 ml of Clear-Sol I, the radioactivity of the effluent perfusate was measured in a scintillation counter (LSA-500, Beckman Coulter, Inc., CA). The outflow patterns were analyzed by statistical moment analysis. In brief, the AUC and mean residence time (MRT) were calculated as follows:

$$\mathrm{AUC} = \int_0^\infty C dt \quad (3)$$

$$\mathrm{MRT} = \int_0^\infty tCdt/\mathrm{AUC} \quad (4)$$

where t is the time and C is the concentration of ^{32}P-labeled galactosylated lipoplex. The moments can be calculated by numerical integration using a linear trapezoidal formula and extrapolation to infinite time based on a monoexponential equation (Yamaoka et al., 1978). The t values were corrected for the lag time of the catheter. The recovery ratio (F) and extraction ratio (E) were derived from $F = \mathrm{AUC} \cdot Q$ (flow rate) and $E = 1 - F$, respectively.

The outflow patterns were also analyzed based on a two-compartment dispersion model, where sinusoidal and binding compartments were considered. The mass balance equations involving the axial dispersion in the sinusoidal space are as follows:

$$\frac{\partial C_S(t,z)}{\partial t} + v\frac{\partial C_S(t,z)}{\partial z} = D\frac{\partial^2 C_S(t,z)}{\partial z^2} - k_{12} \times C_S(t,z) + \varepsilon k_{21} \times C_B(t,z) \quad (5)$$

$$\frac{\partial C_B(t,z)}{\partial t} = \frac{1}{\varepsilon} k_{12} \times C_S(t,z) - k_{21} \times C_B(t,z) - k_{int} \times C_B(t,z) \quad (6)$$

where $C_S(t, z)$ and $C_B(t, z)$ are the concentrations of drug in the sinusoidal space and binding compartment, respectively, D is the dispersion coefficient, ϵ is the volume ratio of the binding compartment to the sinusoidal space in the liver, k_{12} and k_{21} are the forward and backward partition rate constants between the sinusoidal space and binding compartment, k_{int} is the first-order internalization rate constant from the binding compartment to the intracellular space, v is the linear flow velocity of the perfusate, t is time, and z is the axial coordinate in the liver. The initial and boundary conditions are given as follows:

$$C_S(t, 0) = M/Q \times f_I(t),\ C_S(0, z) = 0,\ C_S(t, \infty) = 0,\ C_B(t, 0) = 0,\ C_B(0, z) = 0 \quad (7)$$

where M is the amount of drug injected into the liver, Q is the flow rate of the perfusate, and $f_I(t)$ has the dimension of the reciprocal of time. Taking the Laplace transform with respect to t, rearranging, substituting the length of the sinusoidal space L with z, and introducing the cross-sectional area of the sinusoidal space A, the following image equation is obtained as follows:

$$\tilde{C}_S(s) = \frac{M}{Q}\tilde{f}_I(s);\ \exp\left[\left\{\frac{Q}{2D_C} - \sqrt{\left(\frac{Q}{2D_C}\right)^2 + \frac{1}{D_C}\left\{s + k_{12} - \frac{k_{12} \times k_{21}}{s + k_{21} + k_{int}}\right\}}\right\}V_S\right] \quad (8)$$

where $\tilde{C}_S(s)$ and $\tilde{f}_I(s)$ denote the Laplace transform of the concentration in the venous outflow and input function $f_I(t)$, respectively, D_C is the corrected dispersion coefficient ($D_C = D \cdot A^2$), V_S is the sinusoidal volume (= L · A), and the flow rate Q is equal to A × v.

Each parameter (D_C, k_{12}, k_{21}, k_{int}, and V_S) was calculated by curve-fitting of the Laplace-transformed equation to the experimental venous outflow pattern using a nonlinear least-squares program with a fast inverse Laplace transform algorithm MULTI (FILT) (Yano et al., 1989). The damping Gauss-Newton method with no constraint was used for curve-fitting with the MULTI algorithm. Herein, $f_I(t)$ was assumed to be a Δ function, because the lipoplexes were rapidly injected using a six-rotary valve injector.

For evaluation of the intrahepatic localization of the amounts taken up, 30 min after injection of ^{32}P-labeled galactosylated lipoplex into the isolated perfused liver, the radioactivities in the liver PC and NPC were separately determined after centrifugal separation of PC and NPC in collagenase-digested liver as described previously (Fumoto et al., 2003b).

Observation of Dissociation of pDNA and Lipids from Lipoplex Induced by Mixing with Blood. Carboxy-fluorescein labeling of pDNA was performed using the Label IT Fluorescein Nucleic Acid Labeling Kit (Mirus Co., Madison, WI). Liposomes were labeled with Rh-DOPE at 2% (mol/mol) total lipid. Fluorescent-labeled lipoplex was then prepared by mixing fluorescein-labeled pDNA with rhodamine-labeled liposomes as described above. To observe the dissociation of pDNA and lipids from lipoplex induced by whole blood, fluorescent-labeled lipoplex was mixed with 30% blood and subsequently centrifuged and the erythrocytes were washed twice with phosphate-buffered saline. To investigate the effect of

TABLE 1
Effect of preincubation with serum on the particle size and ζ potential of galactosylated lipoplex
Results are expressed as the mean ± S.D. of three experiments. Statistical comparisons were performed using an unpaired Student's t test.

Incubation	Mean Particle Size	ζ Potential
	nm	*mV*
None (control)	142.1 ± 7.20	35.8 ± 5.67
With serum	217.5 ± 1.08*	−16.2 ± 3.20*

* $P < 0.01$.

preincubation with serum, fluorescent-labeled lipoplex was mixed with 15% serum for 5 min and then mixed with 15% erythrocyte suspension to adjust the hematocrit. Lipoplex integrity was assessed by fluorescent resonance energy transfer (FRET) from fluorescein-pDNA to rhodamine lipids. Precipitates (i.e., lipoplex bound to blood cells) were mounted on glass slides, covered by slips, and observed by confocal laser-scanning microscope (MRC 1024; Bio-Rad, Hercules, CA). On the other hand, galactosylated lipoplex in the supernatant was measured by spectrofluorophotometry (RF540; Shimadzu Co., Kyoto, Japan). The excitation wavelengths were 480 and 550 nm for fluorescein pDNA and Rh-DOPE.

Agarose Gel Electrophoresis. The pDNA stability of the galactosylated lipoplex in blood was determined by agarose gel electrophoresis (Harvie et al., 2000). The galactosylated lipoplex was preincubated with blood components at 37°C. After incubation, pDNA was extracted from the mixture by phase separation using phenol/chloroform/isoamyl alcohol (25:24:1) followed by precipitation with ethanol. Precipitated pDNA was redissolved with Tris borate-EDTA buffer, pH 8.0, and subjected to agarose gel electrophoresis. Densitometric analysis was performed using a commercially available computer program [CS analyzer; Atto Bioscience and Rise Corporation, Sendai, Japan].

Serum IFN-γ Concentration Measurement. Blood was collected 6 h after intraportal injection of galactosylated lipoplex, simultaneously with the in vivo transfection experiment, and was subsequently allowed to stand for 3 h at 4°C. Serum was collected after centrifugation and frozen at −80°C until measurement. The serum IFN-γ concentration was determined using commercially available enzyme-linked immunosorbent assay kits (OptEIA mouse IFN-γ set; BD Biosciences, San Jose, CA).

Statistical Analysis. Statistical comparisons were performed by an unpaired Student's t test for two groups or Dunnett's test for multiple comparisons with a control group. Statistical comparisons in the transfection experiments and serum IFN-γ measurements were performed by the Mann-Whitney test for two groups or Steel's test for multiple comparisons with a control group because of the heterogeneity of the variance evaluated by the F test and Bartlett test, respectively.

Results

Effect of Blood Components on the Physicochemical Characteristics of Galactosylated Lipoplex. To investigate the effect of serum protein on the physicochemical characteristics of galactosylated lipoplex, the particle size and ζ-potential were measured after exposure to mouse serum because these parameters affect the hepatic disposition of galactosylated lipoplex (Fumoto et al., 2003b). Mixing with serum [30% (v/v)] significantly enlarged the particle size of the lipoplex (Table 1). The ζ-potential of the galactosylated lipoplex was significantly reduced by mixing with serum, and the charge became negative, suggesting that negatively charged serum proteins covered much of the galactosylated lipoplex surface. These results are consistent with our previous report about the conventional lipoplex (Sakurai et al., 2001a).

After mixing galactosylated lipoplex with erythrocyte suspension, hemagglutination was observed. However, mixing galactosylated lipoplex with whole blood did not induce any obvious hemagglutination (data not shown), suggesting that the presence of serum components prevents hemagglutination. Recently, Eliyahu et al. (2002) also reported similar results with the conventional lipoplex. Thus, galactosylated lipoplex was mixed with whole blood to evaluate the effect of blood cells on transfection activity.

Transfection Activities of Galactosylated Lipoplex Preincubated with Blood Components. To study the effect of blood components on in vivo transfection activity, galactosylated lipoplex was preincubated with serum or whole blood before administration and the transfection activities in the liver were evaluated 6 h after intraportal injection to mice. When the galactosylated lipoplex was preincubated with serum, the hepatic transfection activities were enhanced approximately 20- to 70-fold (Fig. 1A). However, incubation with whole blood [30% (v/v)] reduced the transfection activity in the liver by 97% (Fig. 1B). These results show that the interaction with blood cells markedly inhibits the hepatic transfection activity of galactosylated lipoplex. In addition, higher concentration of blood components exhibited

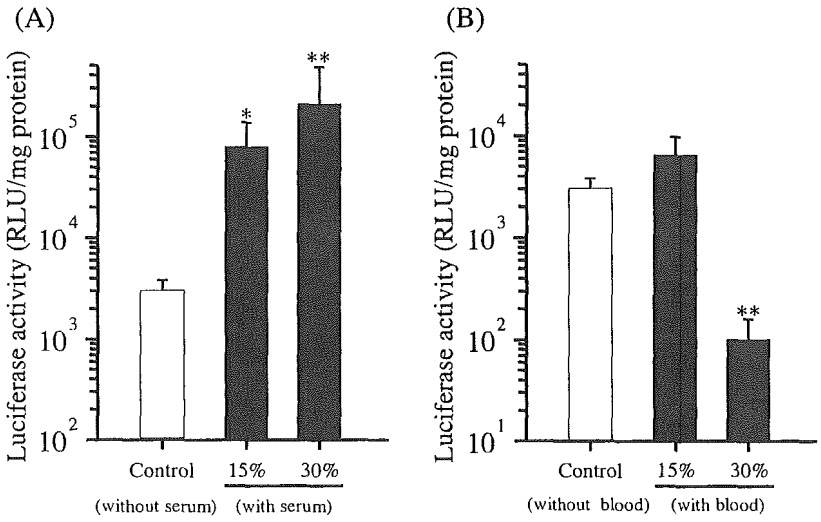

Fig. 1. Effect of preincubation with serum (A) or whole blood (B) on the hepatic transfection activity of galactosylated lipoplex after intraportal injection in mice. pDNA (30 μg) was complexed with galactosylated liposomes at a charge ratio of +2.3. Five minutes before injection, the lipoplexes were mixed with serum or whole blood at the indicated volume ratio. Luciferase activity was determined 6 h postinjection of the lipoplex. Each value represents the mean ± S.D. of at least three experiments. Statistical comparisons with the control group were performed by Steel's test (*, $P < 0.05$; **, $P < 0.01$). RLU, relative light unit.

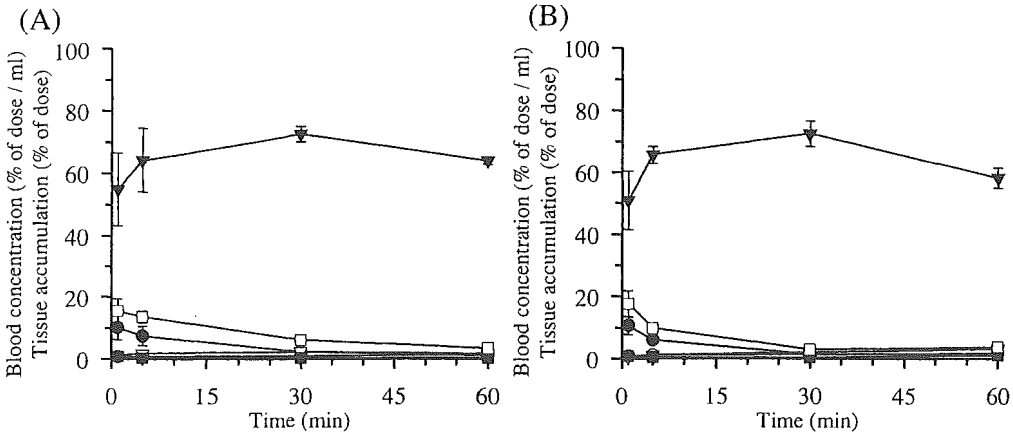

Fig. 2. Effect of preincubation with serum on the distribution of galactosylated lipoplex after intraportal injection in mice. [^{32}P]pDNA (30 μg) was complexed with galactosylated liposomes at a charge ratio of +2.3. Five minutes before injection, galactosylated lipoplex was mixed without (A) or with (B) 30% serum. Radioactivities were determined in the blood (●), lung (□), liver (▼), kidney (○), spleen (▽), and heart (■). Each value represents the mean value ± S.D. of at least three experiments.

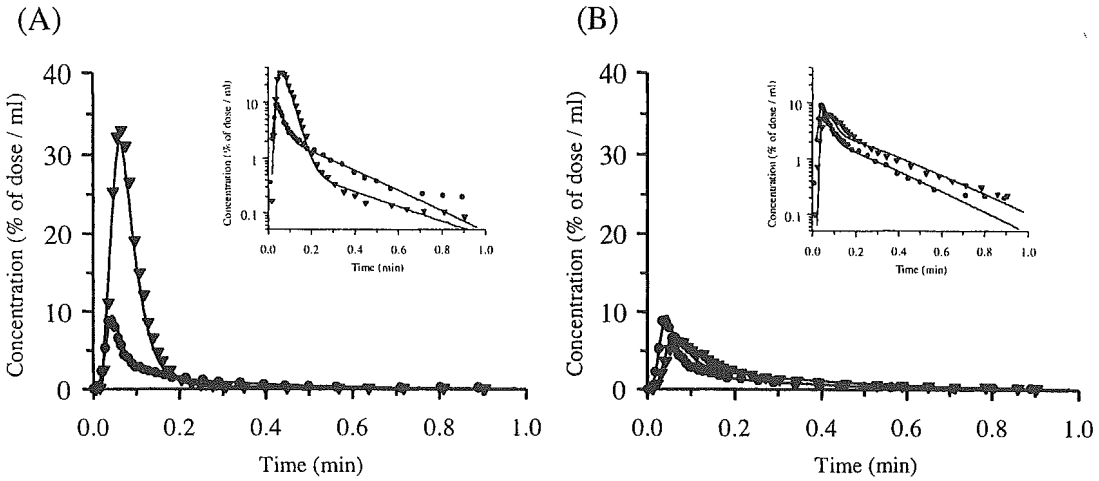

Fig. 3. Typical venous outflow patterns of ^{32}P-labeled galactosylated lipoplex with 30% serum (A) and with 30% whole blood (B) in perfused rat liver. The insets show semilogarithmic plots. The curves simulated by a two-compartment dispersion model are also shown in these figures. Circle symbols represent control, and inverted triangles represent incubation with serum (A) or whole blood (B).

more marked effect on transfection activity. In in vivo condition, blood volume is larger than the volume of the lipoplex solution. Thus, the result of 30% blood or serum would be more close to in vivo condition than the result of 15% blood components. Therefore, we applied 30% blood components as the experimental condition for further studies.

In Vivo Distribution of Galactosylated Lipoplex Preincubated with Serum. To investigate why the transfection activity of galactosylated lipoplex was enhanced by incubation with serum, the biodistribution of galactosylated lipoplex preincubated with serum was evaluated using ^{32}P-labeled galactosylated lipoplex (Fig. 2). However, similar distribution patterns

TABLE 2

Effect of incubation with serum or whole blood on the moment parameters for galactosylated lipoplex in the liver perfusion experiments

Results are expressed as the mean ± S.D. of three experiments. Statistical comparisons with the no incubation group were performed by Dunnett's test.

Incubation	AUC	MRT	E
	% of dose · s/ml	*s*	*%*
None (control)	62.0 ± 5.05	14.9 ± 1.03	87.0 ± 1.04
With serum	177 ± 13.9*	7.96 ± 0.56*	65.3 ± 1.94*
With whole blood	79.4 ± 2.43	18.6 ± 2.95	83.2 ± 1.22**

* $P < 0.01$; ** $P < 0.05$.

TABLE 3

Effect of incubation with serum or whole blood on the model parameters for galactosylated lipoplex in the liver perfusion experiments

Results are expressed as the mean ± S.D. of three experiments. Statistical comparisons with the no incubation group were performed by Dunnett's test.

Incubation	k_{12}	k_{21}	k_{12}/k_{21}	k_{int}
	min^{-1}			*min^{-1}*
None (control)	33.9 ± 4.33	1.68 ± 0.35	20.4 ± 2.31	3.88 ± 0.43
With serum	14.5 ± 1.12*	0.27 ± 0.04*	53.8 ± 2.98*	3.02 ± 0.06**
With whole blood	28.8 ± 2.39	3.63 ± 0.30*	8.00 ± 1.36*	4.22 ± 0.35

* $P < 0.01$; ** $P < 0.05$.